Rotational-state-selective field ionization of molecular Rydberg states

R. Patel, N. J. A. Jones, and H. H. Fielding
Department of Chemistry, University College London, 20 Gordon Street, London WC1H 0AJ, United Kingdom
(Received 2 May 2007; revised manuscript received 16 July 2007; published 12 October 2007)

This paper presents state-selective field ionization spectra of highly excited Rydberg states of NO. The competition between electron-nuclear coupling and electron-field coupling is investigated and it is shown that the slew rate of the electric field can be exploited to control the rotational quantum state composition of field-ionized molecules.

DOI: 10.1103/PhysRevA.76.043413 PACS number(s): 33.80.Rv, 33.55.Be

I. INTRODUCTION

Selective field-ionization (SFI) has been exploited widely as an experimental tool to measure the composition and character of highly excited Rydberg states of atoms. In SFI, a ramped electric field applied to a Rydberg atom has the effect of creating a saddle point in the Coulomb potential and lowering the classical ionization limit, which eventually leads to ionization. The mechanism of field ionization, and hence the field at which a particular Rydberg state is ionized, is highly dependent on the rate at which the electric field is increased; however, atoms in different Rydberg states tend to ionize at different fields, so it is possible to identify Rydberg states by their field-ionization signal. There have been numerous investigations of SFI mechanisms in atomic Rydberg systems [1,2], in particular Na [1,3] and the heavier alkali metals Rb and Ce [4–6]. SFI has been applied to infer Rydberg state populations from ionization signals in various wave packet experiments [3,7,8], e.g., to determine the amplitude of shaped wave packets in Ce [7] and to assess fitness in a coherent control experiment in Na [3]. It has been shown that changing the shape of the ramped field can improve the selectivity of field ionization, e.g., Ref. [6]. Shaped SFI ramps have also proved a useful tool in pulsed-field ionization zero-kinetic energy (PFI-ZEKE) photoelectron spectroscopy [4,9,10]. In the context of ZEKE spectroscopy, there have been several investigations of the effects of electric fields on the lifetimes of very high molecular Rydberg states [10,11]. However, the dynamics of SFI of molecular Rydberg states has not been investigated.

In a molecular Rydberg system, there are Rydberg series converging to each rovibronic state of the ion, and not only is the density of states very high but these series interact with one another, leading to a very complex and irregular Rydberg spectrum. On the application of a slow rising electric field pulse, the field-ionization routes become more complicated than in an atomic system because there is the additional possibility of transferring populations between Rydberg series associated with different rotational states of the ion core.

To understand the mechanism of SFI requires an understanding of the evolution of Rydberg states from zero field to high field. Turning on an external electric field breaks the spherical symmetry of the Rydberg system and mixed orbital angular momentum states with $\Delta l = \pm 1$. Although l is no longer a good quantum number, the Schrödinger equation is separable but requires a transformation to parabolic coordinates and the introduction of a quantum number $k = -n+1, -n+3, \ldots, n-1$ to label the parabolic eigenstates. The frequencies of these Stark states (to first order) are

$$\omega_{nk} = -1/2n^2 + 3nkF/2. \tag{1}$$

The high angular momentum states ($l \geqslant 3$) that are nearly degenerate in zero field, fan out almost linearly with increasing field until neighboring n manifolds cross ($F = 1/3n^5$). In nonhydrogenic atoms or molecules, all the levels of the manifold are coupled by the finite size of the ionic core and form multilevel avoided crossings (or Landau-Zener crossings) in the region $F > 1/3n^5$. When the electric field is ramped, the mechanism by which these avoided crossings are traversed depends on the speed at which they are approached, which in turn depends on the gradients of the potential curves, dE/dF, and the slew rate of the electric field, dF/dt. The probability of making a diabatic transition is approximately [12]

$$P_{diabatic} = \exp\left[\frac{2\pi|V_{12}|^2}{|dE_1/dF - dE_2/dF|dF/dt}\right], \tag{2}$$

where V_{12} is the coupling matrix of the interaction causing the avoided crossing and the separation of states at the crossing $W_{12} = 2V_{12}$ (all quantities in atomic units). The rate of change of the energy separation is, $dW_{12}/dt = |dE_1/dF - dE_2/dF|dF/dt$. For slow enough slew rates (a few hundred V cm^{-1} μs^{-1}), the preferential route to the ionization continuum tends to be via the adiabatic path, in which case the electron is ionized at the classical field-ionization threshold, $F = 1/16n^4$. For rapid slew rates (a few hundred V cm^{-1} ns^{-1}), the system tends to follow the diabatic path and the electron is ionized at the higher field strength, $F = 1/9n^4$.

In a Rydberg molecule, there are series of Stark manifolds, $n(N^+)$, associated with each rotational state of the molecular ion, N^+, each of which is independently characterised by its own adiabatic and diabatic field-ionization thresholds. Furthermore, manifolds associated with different rotational states that are coupled by zero-field core interactions will form additional avoided crossings, opening up the possibility for population to be transferred adiabatically from one rotational quantum state to another.

In this paper, we investigate SFI of highly excited Rydberg states of NO in a densely populated region of the spectrum below the first ionization limit, and probe the competi-

tion between electron-nuclear coupling and electron-field coupling. We demonstrate that the slew rate of the electric field can be used as a control parameter for steering molecules prepared in one rotational quantum state into molecular ions in different rotational quantum states, i.e., to control the field-ionization product. This type of quantum control of highly electronically excited molecules contrasts with coherent control, which is based on interfering optical pathways, and has analogies with dynamic Stark control of lower electronically excited states of molecules using strong fields [13].

II. EXPERIMENT

NO is a model Rydberg molecule because it has a closed shell ionic core, which simplifies the angular momentum coupling, and a low ionization limit which allows relatively easy access to the Rydberg states by two-photon excitation. The Rydberg states of NO are well characterized due to early absorption studies by Miescher [14,15]. Since then, the spectroscopy of the bound, autoionizing and predissociating Rydberg states of NO has been investigated in further detail by several groups [16–20] and there has been a great number of theoretical studies of these Rydberg states, e.g., Refs. [16,17,20,21]. Experimental observations of molecular Rydberg wave packets were carried out in NO [22,23], as were demonstrations of coherent control in a Rydberg molecule [24]. NO also remains one of the few molecules whose Rydberg states have been investigated experimentally in the frequency domain in the presence of a dc electric field. Goodgame *et al.* [25] investigated the Stark effect on low ($n=10-20$) autoionizing Rydberg states of NO converging to the $v^+=1$ ionization limit, and Vrakking *et al.* [26] reported a detailed study of the Stark effect in very high ($n=40-120$) Rydberg states converging to the $v^+=0$ ionization limit. Warntjes *et al.* [27] also investigated Rydberg states converging to the $v^+=0$ ionization limit, but above the field-ionization limit. In a recent paper, we presented a detailed experimental and theoretical investigation of intermediate Rydberg states ($n=25-32$) converging to the $v^+=0$ ionization limit well below the field ionization threshold in dc fields in the range $0-120$ V cm^{-1}. This work extends these investigations to ramped electric fields.

Rydberg states converging to the $v^+=0$ ionization limit are accessed by double resonance excitation through a specific rovibrational level of the A $^2\Sigma^+$ state of NO (Fig. 1). The experiment employs two nanosecond dye lasers pumped by a single Nd:YAG laser operating at 20 Hz. The frequency-tripled output of the first dye laser is used to excite the $A\,^2\Sigma^+(v'=0,N'=2,J'=\frac{5}{2}) \leftarrow X\,^2\Pi_{3/2}(v''=0,J''=\frac{7}{2})$ transition at 44 085.59 cm^{-1}. Rydberg states converging to the $X\,^1\Sigma^+$ ionization limits of NO^+ are accessed from the intermediate A state using the frequency-doubled output (325–330 nm) of the second dye laser. The output energies of the two lasers are both around 15 mJ/pulse, and the bandwidths of both are approximately 0.05 cm^{-1}. The two laser beams are combined at a dichroic mirror and focused into a pulsed, skimmed, molecular jet of NO between a pair of electric field plates separated by 1 cm. After a 70 ns delay, a ramped electric field (2 kV cm^{-1} with a variable rise time of 20–2000 ns) ionizes the Rydberg states. The polarizations of the electric field vectors of both laser pulses are parallel to the pulsed electric field. The field-ionized electrons are pushed towards a multichannel plate detector placed approximately 2 cm away from the interaction region. The amplified electron signal is recorded by a digital oscilloscope, summed over 1000 laser shots and stored, with the SFI field profile, on a computer.

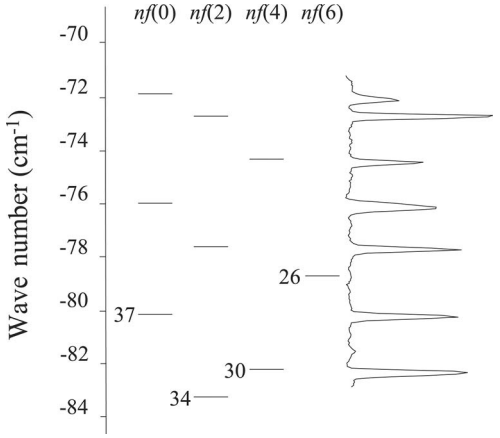

FIG. 1. An energy level diagram showing the interleaved $f(N^+)$ Rydberg series accessible from the A $^2\Sigma^+$ ($v'=0$, $N'=2$, $J'=\frac{5}{2}$) state of NO, together with a portion of the corresponding 1+1 resonance-enhanced multiphoton ionisation spectrum. The vertical scale represents binding energy with respect to the $N^+=0$ ionization limit.

A portion of the Rydberg spectrum, obtained by collecting the total electron yield as a function of the wave number of the second laser is plotted in Fig. 1. The angular momentum coupling in the ground state of NO is intermediate between Hund's case (a) and (b). In this intermediate coupling scheme, each rotational state is split into two spin-orbit components, with $\Omega=1/2$ and $\Omega=3/2$. These states are labeled $^2\Pi_{1/2}$ and $^2\Pi_{3/2}$. The lower rotational levels are well described using Hund's case (a) coupling, whereas higher rotational levels tend to Hund's case (b). As the two spin-orbit states are only separated by 124 cm^{-1}, rotational levels of both the $^2\Pi_{1/2}$ and $^2\Pi_{3/2}$ states are populated in our molecular beam. Here we use a transition from the $^2\Pi_{3/2}$ ground state. The A $^2\Sigma^+$ state is the lowest Rydberg state of NO and is predominantly a $3s\sigma$ Rydberg state [28]. The most appropriate angular momentum coupling scheme to describe this state is Hund's case (b), and each rotational level N' is split by spin-rotation coupling into two levels, $J'=N'+1/2$ and $J'=N'-1/2$, with even and odd parity, respectively. In this work, the intermediate level we use is $v'=0$, $N'=2$, $J'=5/2$, which has even parity.

The Rydberg series accessed from the A-state are labeled using the notation $nl(N^+)$, where n is the principal quantum number, l is the orbital angular momentum quantum number, and N^+ is the rotational quantum number of the molecular ion core. The most appropriate coupling scheme for these Rydberg states is Hund's case (d). The total angular momentum of the Rydberg system is given by $\mathbf{J}=\mathbf{N}^+ + \mathbf{l} + \mathbf{s}$, where $\mathbf{s}$ is the spin angular momentum of the Rydberg electron and the parity of the Rydberg state is $p_{Ryd}=(-1)^{N^++l}$. Conserva-

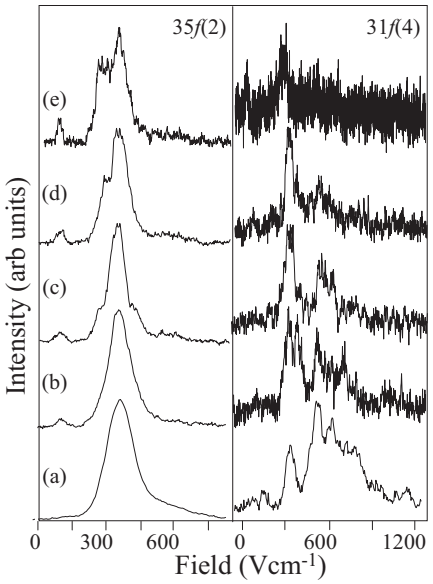

FIG. 2. Measured SFI signals of the $35f(2)$ and $31f(4)$ Rydberg states of NO at slew rates of (a) 6.9, (b) 3.7, (c) 2.8, (d) 2.3, and (e) 1.3 V cm^{-1} ns^{-1}.

tion of angular momentum requires $\mathbf{J}'+\boldsymbol{\gamma}=\mathbf{N}^+ + \mathbf{1}+\mathbf{s}$, where $\boldsymbol{\gamma}$ is the angular momentum of the photon. The electron spin remains the same during a transition from the A-state to a Rydberg state, which leads to $\mathbf{N}'+\boldsymbol{\gamma}=\mathbf{N}^+ + \mathbf{1}$, and there is a requirement for a change in overall parity, $p_{Ryd}p'=-1$. Taking into account the angular momentum composition of the A-state, which is 94% *s* and 5% *d*, [28] and the selection and propensity rules, we expect to access $p(0)$, $p(2)$, $p(4)$, $f(0)$, $f(2)$, $f(4)$, $f(6)$ Rydberg series from the $v'=0$, $N'=2$, $J'=5/2$ intermediate. Weak transitions from the 1% *p* component of the A-state to *s* and *d* series are also possible and have been observed, e.g., Ref. [23]. Vibrational transitions are controlled by the fact that the overriding Franck-Condon factor is for $\Delta v=0$ transitions due to the similarity in potential energy surfaces for the Rydberg and A-state.

In our zero-field spectra, the dominant Rydberg series observed are *f* in character [29]. The *np* Rydberg series are known to rapidly predissociate and will have almost completely decayed on our detection timescale. So while the dominant transition is to the *np* Rydberg states, these are not detected in the current scheme. The predissociating Rydberg states of NO have been studied in detail by Fuji and Morrita [18] and others [30], revealing a rotational dependence of the predissociation lifetime as well as confirming calculations that the *np* states predissociate more rapidly than other orbital angular momentum states [20,31].

III. RESULTS AND DISCUSSION

SFI profiles of two Rydberg states, $35f(2)$ and $31f(4)$, are presented in Fig. 2 for ramped fields with slew rates in the range 6.9 V cm^{-1} ns^{-1} (a) to 1.3 V cm^{-1} ns^{-1} (e). The *f* states have very small quantum defects (~0.01) [15,16,32] and are mixed rapidly into their adjacent Stark manifolds even in weak fields. As the ramped electric field is applied, population placed initially in one $nf(N^+)$ Rydberg state will follow the path of the lowest energy Stark state of the $n(N^+)$ manifold until it crosses an adjacent manifold. The first avoided crossing takes place with the highest energy Stark state of a manifold associated with a different rotational state, and from this point on, the ionization path is determined by the slew rate and the strength of the coupling between the two states [Eq. (2)].

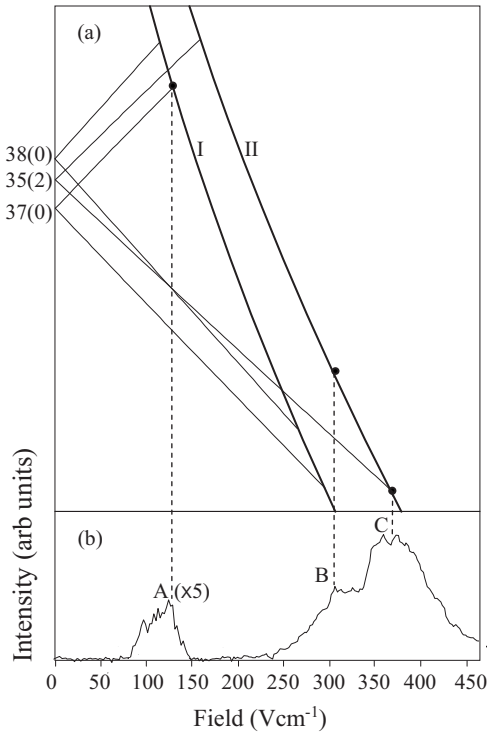

FIG. 3. (a) Extreme members of the $m=0$ hydrogenic Stark manifolds for 37(0), 35(2), and 38(0) high-*l* Rydberg states, calculated using first-order perturbation theory. Curves I and II represent the classical field-ionization limits, $E=B_0N^+(N^++1)-6.12\sqrt{F}$, of the $N^+=0$ and $N^+=2$ Rydberg series, respectively. (b) SFI profile of the $35f(2)$ Rydberg state with a slew rate of 2.3 V cm^{-1} ns^{-1}.

Consider the SFI profile of the $35f(2)$ state with a slew rate of 6.9 V cm^{-1} ns^{-1} [Fig. 2(a)]. Most of the molecules ionize when the field is ~370 V cm^{-1}, which corresponds to diabatic ionization into the $N^+=2$ continuum. When the slew rate is decreased to 3.7 V cm^{-1} ns^{-1} [Fig. 2(b)], an additional peak appears in the SFI profile at ~120 V cm^{-1} and this peak grows as the slew rate is decreased further [Fig. 2(c)–2(e)]. At 2.8 V cm^{-1} ns^{-1} [Fig. 2(c)] a shoulder begins to appear on the low field side of the diabatic peak at ~370 V cm^{-1} and becomes more pronounced as the slew rate is further decreased [Fig. 2(d) and 2(e)]. These features can be explained most easily with the aid of a Stark energy level diagram. In Fig. 3 the extreme members of the $m=0$ hydrogenic Stark manifolds, calculated by first-order perturbation theory [Eq. (1)], are plotted for the 37(0), 35(2), and 38(0) states. The classical field-ionization wave numbers, $E=B_0N^+(N^++1)-6.12\sqrt{F}$, are plotted for adiabatic ionization into $N^+=0$ and $N^+=2$ continua. $B_0=1.988$ cm^{-1} is the rotational constant, and F is in units of V cm^{-1}. A detailed Stark map for NO is calculated for states in the vicinity of the first

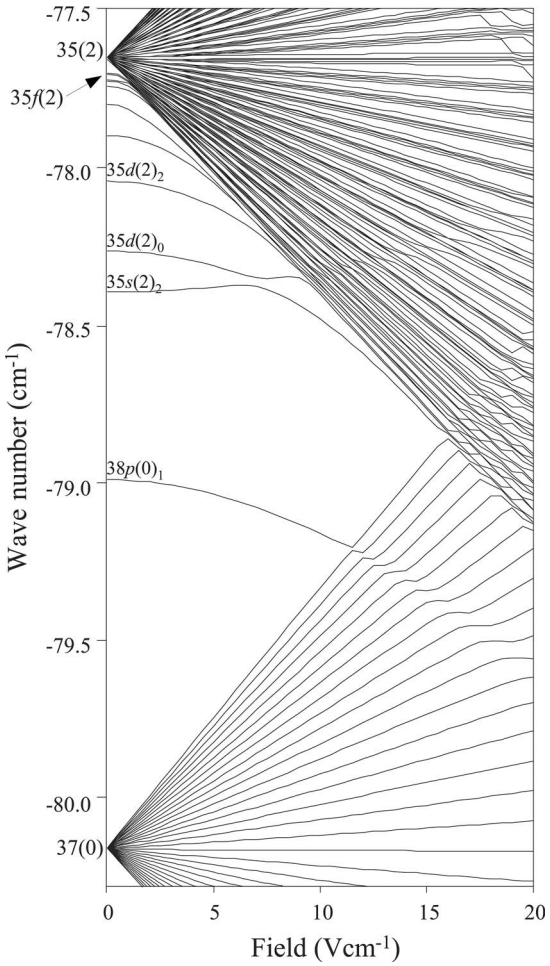

FIG. 4. Stark map for states in the vicinity of the first avoided crossing in the field strength region of 0–20 V cm^{-1}, calculated using a hybrid MQDT and matrix-diagonalization method [29]. The zero-field nondegenerate states are labeled using the $nl(N^+)_N$ notation, where n is the principal quantum number, l is the electron orbital angular momentum, N^+ is the ion core rotational quantum number, and N is the total angular momentum excluding spin, $\mathbf{N}=\mathbf{N}^+ + \mathbf{1}$.

avoided crossing, using the matrix-diagonalization method employed in our earlier work [29] (Fig. 4). As the field is ramped up, the $35f(2)$ state mixes into the 35(2) manifold almost immediately, and the population follows the lowest energy states of the 35(2) Stark manifold until it reaches an avoided crossing with the 37(0) manifold at ~16.7 V cm^{-1}, which arises due to a zero-field coupling between rotational states with $\Delta N^+ = \pm 2$. For the fastest slew rate, the population continues on the diabatic path to the $N^+=2$ classical field-ionization limit at ~370 V cm^{-1} (peak C). At 3.7 V cm^{-1} ns^{-1} [Fig. 2(b)] most of the population still makes this crossing diabatically, although a measurable fraction crosses adiabatically onto the highest energy Stark state of the 37(0) manifold, where it is then transferred diabatically to the $N^+=0$ continuum (peak A in Fig. 3). As the slew rate decreases further, the probability of adiabatic transfer is enhanced and this feature gains intensity. At 2.8 V cm^{-1} ns^{-1} [Fig. 2(c)], a broad shoulder emerges at fields 250–340 V cm^{-1} and becomes more pronounced as the field is increased. We have interpreted this in terms of an increasing number of adiabatic crossings on the route to the $N^+=2$ classical field-ionization limit.

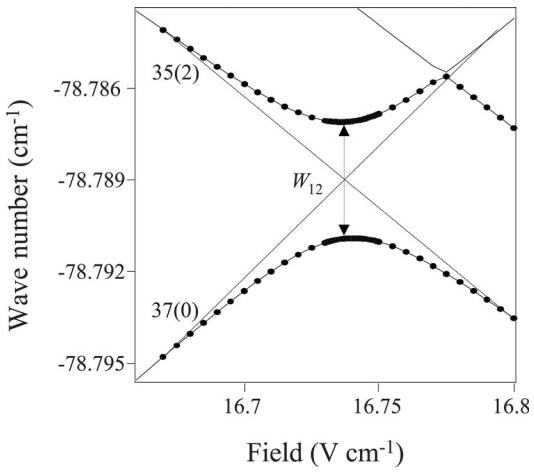

FIG. 5. The first avoided crossing between the $35f(2)$ Stark state with the highest energy Stark state of the 37(0) manifold at ~16.7 V cm^{-1}, calculated using a hybrid MQDT and matrix-diagonalization method [29]. The probability of crossing an isolated avoided crossing diabatically is determined using the Landau-Zener approximation [Eq. (2)], which takes into consideration the energy separation between the two states at the avoided crossing, W_{12}, and the difference in the diabatic gradients (dashed lines).

The avoided crossing between the $35f(2)$ state and the highest energy Stark state of the 37(0) manifold at ~16.7 V cm^{-1} is enlarged in Fig. 5. The gradients of the diabatic potentials are -0.07 cm^{-1} V^{-1} and 0.08 cm^{-1} V^{-1}, and the energy separation at the avoided crossing $W_{12}=3.8\times10^{-3}$ cm^{-1}. The probability of making this crossing diabatically can be calculated using Eq. (2). At the fastest slew rate of 6.9 V cm^{-1} ns^{-1} [Fig. 2(e)], there is no measurable adiabatic population transfer and the calculated probability, $P_{diabatic}=1.00$. At the slowest slew rate of 1.3 V cm^{-1} ns^{-1} [Fig. 2(e)], the experimentally measured fraction of electrons making the crossing adiabatically and being recorded at ~120 V cm^{-1} is 0.03, which is in good agreement with the probability calculated using Eq. (2), $P_{diabatic}=0.98$.

Now consider the SFI profile of the $31f(4)$ state with the fastest slew rate of 6.9 V cm^{-1} ns^{-1} [Figs. 2(a) and 6]. The molecules ionize over a range of fields from 180–1100 V cm^{-1}. The SFI profile is highly structured and the peaks can be assigned to a number of ionization pathways. The $31f(4)$ state mixes into the 31(4) manifold almost immediately, and as the field is ramped the population follows the lowest energy Stark state of this manifold until it meets the first avoided crossing with the highest energy Stark state of the 38(0) manifold. $\Delta N^+ = \pm 4$ coupling is weak, so the avoided crossing between these two states will be very small and at this slew rate, and in fact for all slew rates employed in this work, there is no evidence for any adiabatic population transfer to $N^+=0$. The next avoided crossing takes place with the highest energy Stark state of the 35(2) manifold at ~24 V cm^{-1}. Zero-field coupling between rotational states with $\Delta N^+ = \pm 2$ is stronger and a fraction of the population is transferred adiabatically to the 35(2) manifold

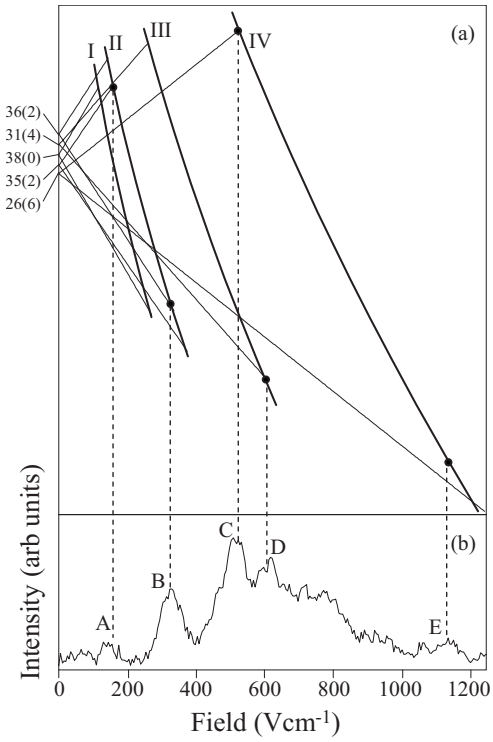

FIG. 6. (a) Extreme members of the $m=0$ hydrogenic Stark manifolds for 26(6), 35(2), 38(0), 31(4), and 36(2) high-l Rydberg states, calculated using first-order perturbation theory. Curves I, II, III, and IV represent the classical field-ionization limits, $E=B_0N^+(N^++1)-6.12\sqrt{F}$, of the $N^+=0$, $N^+=2$, $N^+=4$, and $N^+=6$ Rydberg series, respectively. (b) SFI profile of the $31f(4)$ Rydberg state with a slew rate of 6.9 V cm^{-1} ns^{-1}.

where it continues diabatically to the $N^+=2$ continuum at $\sim$160 V cm^{-1} (peak A). Alternatively, the Rydberg population may cross the interleaved manifolds adiabatically until it crosses onto the lower energy Stark states of the 36(2) manifold where it would then continue diabatically to the $N^+=2$ continuum at $\sim$330 V cm^{-1} (peak B). The population that remained on the lowest energy Stark state of the 31(4) manifold meets the next avoided crossing, with the 26(6) manifold, at $\sim$77 V cm^{-1}. The zero-field coupling between the 31(4) and 26(6) states clearly results in a significant fraction of the population being transferred adiabatically to the highest energy Stark state of the 26(6) manifold, which is then transferred diabatically to the $N^+=6$ ionization continuum at $\sim$525 V cm^{-1} (peak C). This is the most intense peak at the slowest slew rate [Fig. 2(a)]. Peak D is attributed to purely diabatic ionization of $31f(4)$ into the $N^+=4$ ionization continuum at 600 V cm^{-1}. Peak E must arise from population traveling diabatically along the lowest energy Stark state of the 26(6) manifold to the classical field-ionization threshold at 1100 V cm^{-1}. Adiabatic population transfer from the $31f(4)$ to a range of Stark states belonging to the 26(6) manifold gives rise to the SFI signal in the range 600–1100 V cm^{-1}. As the slew rate is decreased [Fig. 2(b)–2(e)], the probability of adiabatic transfer at each of the crossings increases. At the slowest slew rates, the purely adiabatic ionization to the $N^+=4$ continuum (peak B) is the most intense, although there are still some molecules ionizing into $N^+=6$ at $\sim$525 V cm^{-1} (peak C).

IV. SUMMARY

In summary, these detailed investigations of SFI of Rydberg states in a molecule show how the rotational degree of freedom influences the field-ionization pathway. We have shown how the branching ratio between the field-ionization continua associated with different rotational states of the molecular ion is controlled by the slew rate of the electric field. This type of control should prove to be general. In any molecule, the electronic and nuclear degrees of freedom are coupled to some extent, and it is possible to perturb the energy levels and couplings using external electric fields, ranging from the weak ramped fields in this work, to the strong fields associated with intense laser pulses. Future work will aim to investigate the possibility of using shaped electric fields to improve the rotational selectivity and to investigate the prospects of using SFI as a tool to control more molecular phenomena such as the competition between field ionization and predissociation.

ACKNOWLEDGMENTS

We thank the EPSRC for equipment funding and financial support. We are also grateful to R. S. Minns for useful discussions.

[1] T. F. Gallagher, L. M. Humphrey, W. E. Cooke, R. M. Hill, and S. A. Edelstein, Phys. Rev. A **16**, 1098 (1977); T. F. Gallagher, L. M. Humphrey, R. M. Hill, and S. A. Edelstein, Phys. Rev. Lett. **37**, 1465 (1976); T. H. Jeys, G. W. Foltz, K. A. Smith, E. J. Beiting, F. G. Kellert, F. B. Dunning, and R. F. Stebbings, *ibid.* **44**, 390 (1980); J. L. Vialle and H. T. Duong, J. Phys. B **12**, 1407 (1979).

[2] F. G. Kellert, T. H. Jeys, G. B. McMillian, K. A. Smith, F. B. Dunning, and R. F. Stebbings, Phys. Rev. A **23**, 1127 (1981); K. B. Macadam, D. B. Smith, and R. G. Rolfes, J. Phys. B **18**, 441 (1985); J. H. M. Neijzen and A. Donszelmann, *ibid.* **15**, 1981 (1982).

[3] R. E. Carley, E. D. Boleat, R. S. Minns, R. Patel, and H. H. Fielding, J. Phys. B **38**, 1907 (2005).

[4] M. Tada, Y. Kishimoto, M. Shibata, K. Kominato, S. Yamada, T. Haseyama, I. Ogawa, H. Funahashi, K. Yamamoto, and S. Matsuki, Phys. Lett. A **303**, 285 (2002).

[5] F. Robicheaux, C. Wesdorp, and L. D. Noordam, Phys. Rev. A **62**, 043404 (2000); T. F. Gallagher, B. E. Perry, K. A. Safinya, and W. Sandner, *ibid.* **24**, 3249 (1981).

[6] A. Gurtler and W. J. van der Zande, Phys. Lett. A **324**, 315 (2004).

[7] T. C. Weinacht, J. Ahn, and P. H. Bucksbaum, Phys. Rev. Lett. **80**, 5508 (1998).

[8] S. N. Pisharody and R. R. Jones, Phys. Rev. A **65**, 053418 (2002); J. H. Hoogenraad and L. D. Noordam, *ibid.* **57**, 4533

(1998).
[9] G. Reiser, W. Habenicht, and K. Mullerdethlefs, Chem. Phys. Lett. **152**, 119 (1988); U. Hollenstein, R. Seiler, H. Schmutz, M. Andrist, and F. Merkt, J. Chem. Phys. **115**, 5461 (2001).
[10] H. J. Dietrich, K. Muller-Dethlefs, and L. Y. Baranov, Phys. Rev. Lett. **76**, 3530 (1996).
[11] M. Bixon and J. Jortner, J. Chem. Phys. **105**, 1363 (1996); C. Bordas, P. F. Brevet, M. Broyer, J. Chevaleyre, P. Labastie, and J. P. Perrot, Phys. Rev. Lett. **60**, 917 (1988); W. A. Chupka, J. Chem. Phys. **99**, 5800 (1993); **98**, 4520 (1993); S. T. Pratt, *ibid.* **98**, 9241 (1993); W. G. Scherzer, H. L. Selzle, E. W. Schlag, and R. D. Levine, Phys. Rev. Lett. **72**, 1435 (1994); M. J. J. Vrakking and Y. T. Lee, Phys. Rev. A **51**, R894 (1995).
[12] D. A. Harmin and P. N. Price, Phys. Rev. A **49**, 1933 (1994); D. A. Harmin, *ibid.* **56**, 232 (1997); Phys. Rev. Lett. **49**, 128 (1982); Phys. Rev. A **26**, 2656 (1982).
[13] B. J. Sussman, D. Townsend, M. Y. Ivanov, and A. Stolow, Science **314**, 278 (2006).
[14] E. Miescher, Can. J. Phys. **49**, 2350 (1971); J. Mol. Spectrosc. **53**, 302 (1974); **69**, 281 (1978); E. Miescher, Y. T. Lee, and P. Gurtler, J. Chem. Phys. **68**, 2753 (1978).
[15] C. Jungen and E. Miescher, Can. J. Phys. **47**, 1769 (1969).
[16] D. T. Biernacki, S. D. Colson, and E. E. Eyler, J. Chem. Phys. **88**, 2099 (1988).
[17] S. Fredin, D. Gauyacq, M. Horani, C. Jungen, G. Lefevre, and F. Masnouseeuws, Mol. Phys. **60**, 825 (1987).
[18] A. Fujii and N. Morita, Chem. Phys. Lett. **182**, 304 (1991); J. Chem. Phys. **97**, 327 (1992); **98**, 4581 (1993); Laser Chem. **13**, 259 (1994); J. Chem. Phys. **103**, 6029 (1995).
[19] D. Gauyacq, A. L. Roche, M. Seaver, S. D. Colson, and W. A. Chupka, Mol. Phys. **71**, 1311 (1990); S. T. Pratt, C. Jungen, and E. Miescher, J. Chem. Phys. **90**, 5971 (1989).
[20] M. Raoult, J. Chem. Phys. **87**, 4736 (1987).
[21] E. Miescher, Can. J. Phys. **54**, 2074 (1976); D. Uy, C. M. Gabrys, T. Oka, B. J. Cotterell, R. J. Stickland, C. Jungen, and A. Wuest, J. Chem. Phys. **113**, 10143 (2000).
[22] R. A. L. Smith, V. G. Stavros, J. R. R. Verlet, H. H. Fielding, D. Townsend, and T. P. Softley, J. Chem. Phys. **119**, 3085 (2003); R. A. L. Smith, J. R. R. Verlet, E. D. Boleat, V. G. Stavros, and H. H. Fielding, Faraday Discuss. **115**, 63 (2000).
[23] V. G. Stavros, J. A. Ramswell, R. A. L. Smith, J. R. R. Verlet, J. Lei, and H. H. Fielding, Phys. Rev. Lett. **83**, 2552 (1999).
[24] R. S. Minns, R. Patel, J. R. R. Verlet, and H. H. Fielding, Phys. Rev. Lett. **91**, 243601 (2003); R. S. Minns, J. R. R. Verlet, L. J. Watkins, and H. H. Fielding, J. Chem. Phys. **119**, 5842 (2003).
[25] A. L. Goodgame, H. Dickinson, S. R. Mackenzie, and T. P. Softley, J. Chem. Phys. **116**, 4922 (2002).
[26] M. J. J. Vrakking, J. Chem. Phys. **105**, 7336 (1996).
[27] J. B. M. Warntjes, F. Robicheaux, J. M. Bakker, and L. D. Noordam, J. Chem. Phys. **111**, 2556 (1999).
[28] S. N. Dixit, D. L. Lynch, V. McKoy, and Winifred M. Huo, Phys. Rev. A **32**, 1267 (1985); K. Kaufmann, C. Nager, and M. Jungen, Chem. Phys. **95**, 385 (1985).
[29] R. Patel, N. J. A. Jones, and H. H. Fielding, J. Phys. B **40**, 1369 (2007).
[30] L. E. Jusinski, G. E. Gadd, G. Black, and T. G. Slanger, J. Chem. Phys. **90**, 4282 (1989); H. Umemoto and K. Matsumoto, J. Chem. Soc., Faraday Trans. **92**, 1315 (1996).
[31] A. GiustiSuzor and C. Jungen, J. Chem. Phys. **80**, 986 (1984).
[32] E. F. McCormack, F. Di Teodoro, J. M. Grochocinski, and S. T. Pratt, J. Chem. Phys. **109**, 63 (1998).